SMITH-PURCELL FREE ELECTRON LASER WITH BRAGG REFLECTOR*

D.Li[1#], Z. Yang[2], Y. Tsunawaki[3], M. R. Asakawa[4], M. Hangyo[5], S. Miyamoto[6], K.Imasaki[1]
[1] Institute for Laser Technology, Suita, Osaka 565-0871, Japan
[2] University of Electronic Science and Technology of China, Chengdu 610054, China
[3] Osaka Sangyo University, Osaka 574-8530, Japan
[4] Kansai University, Osaka 64-8680, Japan
[5] Osaka University, Suita, Osaka 565-0871, Japan
[6] University of Hyogo, Ako, Hyogo 678-1205, Japan

Abstract

Grating with Bragg reflectors for the Smith-Purcell free-electron laser is proposed to improve the reflection coefficient, resulting in enhancing the interaction of the surface wave with the electron beam and, consequently, relax the requirements to the electron beam. With the help of particle-in-cell simulations, it has been shown that, the usage of Bragg reflectors may improve the growth rate, shorten the time for the device to reach saturation and lower the start current for the operation of a Smith-Purcell free-electron laser.

INTRODUCTION

At the present time, terahertz sources are actively being developed for a variety of applications in biophysics, medical and industrial imaging, nanostructures, and materials science. As a promising alternative in development of a compact, tunable and powerful terahertz source, the Smith-Purcell free-electron laser has attracted many attentions in recent years [1-18].

It is well known that the SP radiation is emitted when an electron passes near the surface of a periodic metallic grating. The wavelength λ of the radiation observed at the angle θ measured from the direction of electron beam is given by

$$\lambda = \frac{L}{|n|}\left(\frac{1}{\beta} - \cos\theta\right) \qquad (1)$$

where L is the grating period, βc the electron velocity, c the speed of light, and n the order of the reflection from the grating. The incoherent SP radiation has been analyzed in many ways, using diffraction theory, integral equation method, and induced surface current model. The superradiant Smith-Purcell radiation is regarded as the result of electron beam bunching, induced by the strong interaction of the continuous beam with the evanescent wave propagating along the grating surface. Several theories have been proposed to explain the superradiant phenomenon and to calculate the growth rate and start current of the radiation [6,7], and some schemes for improving the growth rate and output the radiation are also proposed[12,18].

In this paper, we report the analysis on the Smith-Purcell free-electron laser with using Bragg reflectors.

BASIC THEORY

Typically, Smith-Purcell free-electron laser devices are similar to backward-wave oscillators and travelling-wave tubes, but they use an open grating as the slow-wave structure. It has been shown that the beam interacts with a surface mode of the grating that lies at a wavelength longer than the Smith-Purcell radiation [14-19]. The electron beam interacts with the surface wave for which the phase velocity matches the electron velocity, thus, when the beam current exceeds the so-called start current, strong interaction occurs and the originally continuous electron beam could be periodically bunched by the surface wave and resulting in inducing super-radiant Smith-Purcell radiation[11,12]. However, the super-radiant Smith-Purcell radiation is hard to be observed in experiment because of the stringent requirements to the electron beam [7,9].

Based on the fact that the surface wave cannot radiate and it is partially reflected and partially diffracted at the ends of the grating [11,12], in this paper, a scheme of grating with Bragg reflectors is proposed to improve the reflection coefficient. By such a way, the beam-wave interaction can be enhanced, and then the growth rate could also be improved and, consequently, the start current is expected to be reduced. The Bragg reflector is also formed by open grating, thus, such a configuration adds no impact on the super-radiant Smith-Purcell emission, which emits over the grating at a certain angle.

The surface mode for an open grating as shown in Fig.1, where the grating system is assumed to be perfect conductor, has been well analyzed [19]. According to Floquet's theorem the electric field for the TM wave can be expanded as space harmonics

$$E_x = \sum_{p=-\infty}^{\infty} E_p e^{-\alpha_p y} e^{j(k_p x - \omega t)}\,, \qquad (2)$$

*Work supported by Kurata Grant (1032) and MEXT(No. 22109003)
#dazhi_li@hotmail.com

ISBN 978-3-95450-117-5

where $k_p = k + p\frac{2\pi}{L}$ is the wave number, L the grating period and $\alpha_p^2 = k_p^2 - \frac{\omega^2}{c^2}$. The dispersion equation has been derived out by H. L. Andrews and C. A. Brau [19], and its passive form is written as $\left|R_{mn} - \delta_{mn}\right| = 0$, where

$$R_{mn} = \frac{\tanh(\kappa_n H)}{1+\delta_{m0}} \sum_{p=-\infty}^{\infty} \frac{\kappa_m A}{\alpha_p L} \frac{4}{k_p^2 A^2 - m^2\pi^2} \frac{k_p^2 A^2}{k_p^2 A^2 - n^2\pi^2} \begin{cases} (-1)^m \cos(k_p A) - 1 (m+n=even) \\ j(-1)^m \sin(k_p A) (m+n=odd) \end{cases} \quad (3)$$

,and

$$\kappa_n^2 = (\frac{n\pi}{A})^2 - \frac{\omega^2}{c^2},$$

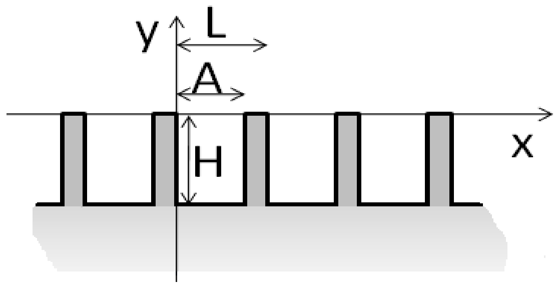

Figure 1: Schematic of an ordinary grating for Smith-Purcell free-electron laser.

where A the width of the groove, and H the depth. With the parameters chosen as L =173 µm, A =62 µm and H =100µm, by numerically solving the equation, the roots give the dispersion relation $\omega(k)$ as shown in Fig.2. The beam line of 35 keV is also plotted, and its intersection with the dispersion curve implies the operation point of the free-electron laser. As is shown, the intersection occurs at the part where the surface wave travels with a positive phase velocity equal to the electron velocity, the group velocity (for the problem of this paper it is equal to energy velocity) is negative, so, the device is in the manner of a backward-wave oscillator. In the following we confine our attention to the backward-wave operation. We know that a surface mode consists of a superposition of an infinite number ($p = -\infty..\infty$) of spatial harmonics, and those with positive k_p carrying energy flows forward, while those with negative k_p flows backward. For the backward-wave part in Fig.2, the total energy-flow is backward and this leads to the negative group velocity. At the central point $kL/2\pi$ =0.5, the group velocity is zero, which means the forward energy-flow is same to the backward one. From

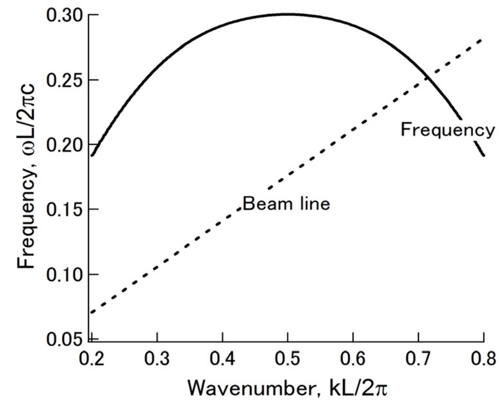

Figure 2: Dispersion relation of the surface wave of a grating. The beam line is for 35 keV electrons. The operation point of the Smith-Purcell free-electron laser is the intersection of the dispersion curve and the beam line.

the dispersion equation, we can calculate relative amplitudes of the first few spatial harmonics (for convenience they are normalized to the zero harmonic of the field in groove. See Eq.18 in Ref[19]), and then calculate the average power carried by each harmonic through the calculation of Poynting vector $S_p^x = \frac{1}{2} E_p^y H_p^z$. The results are as shown in Fig. 3, where we plot the absolute

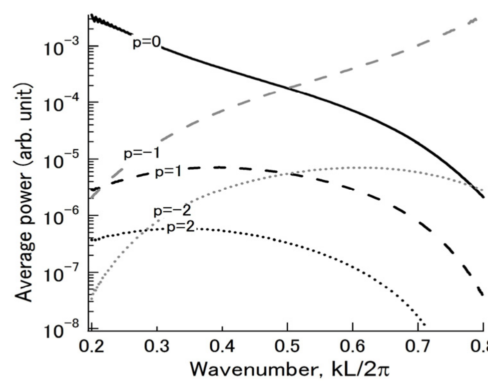

Figure 3: Poynting vectors of the first few harmonics. Note that S_{-1}^x and S_{-2}^x are actually with negative value, meaning that energy flows backward.

value of normalized S_p^x for convenient comparison, and note that S_{-1}^x and S_{-2}^x are actually with negative value, meaning that energy flows backward. As is shown in Fig.3, in the forward-wave region ($kL/2\pi < 0.5$) the zero harmonic carries most of the energy, while in the backward-wave region ($kL/2\pi > 0.5$) the -1th harmonic is dominant. Note that energy exchanges between electron beam and entire harmonics though the beam only synchronize with the zero harmonic.

We are trying to use Bragg gratings as reflectors connected at one end or two ends of the main grating as shown in Fig. 4. For the case of operation point being at

ISBN 978-3-95450-117-5

the backward-wave region, the Bragg reflector may correspond to the zero harmonic or the -1th harmonic. The reflected zero (or -1th) harmonic increases the entire field when the phase is well matched, and certainly this leads to the increase of the field of zero harmonic and, consequently, the beam-wave interaction would be enhanced. We can tune the lengths of g_1 and g_2 as shown in Fig.4 to optimize the phase-matching. In the following, we demonstrate this scheme by a two-dimensional particle-in-cell simulation.

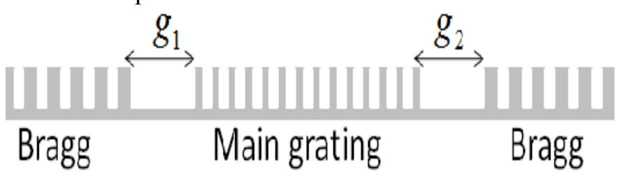

Figure 4: Schematic of Smith-Purcell free-electron laser with Bragg reflectors.

SIMULATION

The simulations are carried out with using CHIPIC code [20], which is a finite-difference, time-domain code designed to simulate plasma physics processes. The grating system is assumed to be perfect conductor as shown in Fig.5, and it has uniform rectangular grooves along the z direction, with parameters mentioned above. The main grating is assumed to have 60.5 periods. A sheet electron beam with the thickness of 24 μm propagates along the x direction, and its bottom is over the grating surface by height of 34 μm. It is a perfect beam produced from a small cathode located at the left boundary of the simulation area. The beam wave interaction and radiation propagation occur in the vacuum box, which is enclosed with absorber regions. Since it is a

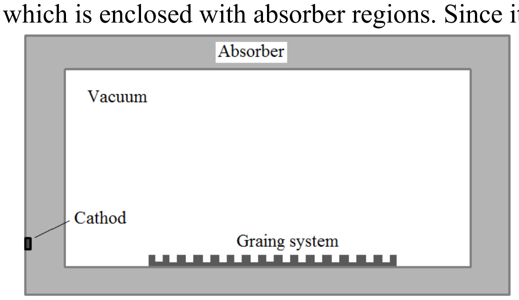

Figure 5: Schematic of simulation box.

two-dimensional simulation, it is assumed that all fields and currents are independent of the z direction. We have simulated the reflection effect of a surface wave by the end of grating and by Bragg grating with using the method mentioned in Ref. [21]. It has been shown that for the frequency of our interest the reflection coefficient can achieve about 0.75 when a Bragg grating with 2.5 periods is connected. Hereafter, we adopt 2.5 periods for the Bragg grating used in the following simulations.

We firstly determine the wavelength of the zero and -1th order harmonic through simulating the main grating alone, and with using 35 keV electron beam it turns out to be $\lambda_0 = 242$ μm and $\lambda_{-1} = 600$ μm, respectively. Thus, the period of the corresponding Bragg grating should be $d_B^0 = \lambda_0/2 = 121$ μm and $d_B^{-1} = \lambda_{-1}/2 = 300$ μm, respectively. We simplify choose the groove width as half the period, and groove depth 100μm same as that of the main grating. The frequency of the surface wave is 427 GHz, which is a little bit lower than that of the analytical calculation, due to the decrease of the electron's energy induced by the effect of space charge [12]. The procedure of optimization is as follows: for the case of reflecting zero harmonic, we firstly set the Bragg grating at the downstream end only, and tune g_2 to find the biggest growth rate through observing the evolution of the z-component magnetic field. The observation point is set 17.3 μm above the grating surface at the centre of the main grating; Next, we set another Bragg grating at the upstream end and optimize g_1. For the case of reflecting -1th harmonic, we have to set the Bragg grating at the upstream end firstly, because it moves backward (negative x direction). The simulation results are shown in Fig. 6, where the evolutions of the z-component magnetic

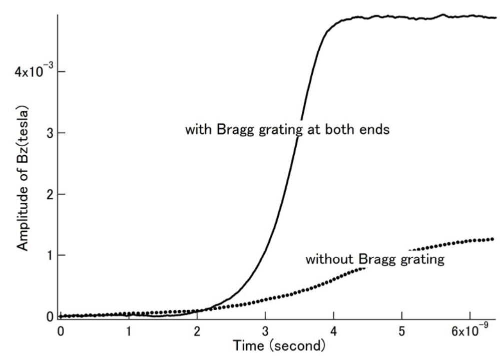

Figure 6: Evolution of the amplitude of z-component magnetic field. Bragg grating with period length d_B^0 are used at both ends, and $g_1 = 0$, $g_2 = 0$. The corresponding elongated grating is with period number of 64.5.

fields are given. For comparison, the results of corresponding elongated grating (without Bragg gratings but with the same overall length) are also plotted. In Fig.6 , results of Bragg grating (used at both ends) with period length of d_B^0 are demonstrated. It is found that for the same current density ($1.8\times10^7\ A/m^2$), oscillation starts earlier when Bragg reflectors are used, and saturation occurs sooner. It is also found that the growth rate is $\mathrm{Im}(\omega) = 2.5\times10^9 s^{-1}$ when Bragg reflectors are used and $\mathrm{Im}(\omega) = 8.2\times10^8 s^{-1}$ when they are not. Bragg reflectors increase the growth rate by a factor of 3. By varying the current density it is found that the start current density is $1.4\times10^7\ A/m^2$ when Bragg reflectors are used and $1.6\times10^7\ A/m^2$ when they are not used. In Fig.7, we show the cases of using Bragg grating (period length d_B^{-1}) upstream alone, both ends and corresponding elongated gratings. It is shown that, when Bragg reflector is used upstream alone, the growth rate is almost same ($\mathrm{Im}(\omega) = 2.3\times10^9 s^{-1}$) to the corresponding elongated grating, but, the oscillation starts earlier when it is used. For the case of using Bragg grating at both ends, by the parameters used in this paper, growth rate and oscillation-starting time are close to those of corresponding elongated grating.

In Fig. 6 and 7, the magnetic field observed at the center of grating and near the grating surface is total field involving all space harmonics. The saturated field is greater with Bragg reflectors, because the corresponding harmonic is reflected back into the grating with higher reflectivity and increase the total field.

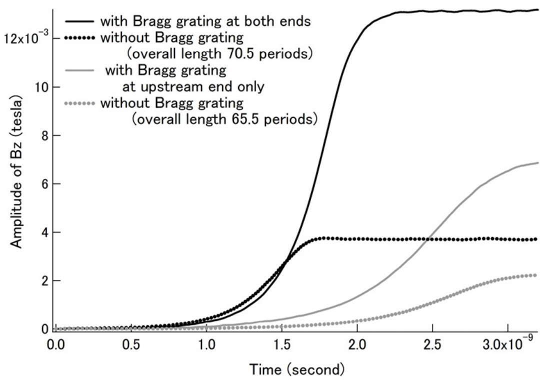

Figure 7: Evolution of the amplitude of z-component magnetic field. Bragg grating with period length d_B^{-1} is used upstream alone ($g_1 = 0.5d_B^{-1}$), and both ends ($g_1 = 0.5d_B^{-1}$, $g_2 = 0$).The corresponding elongated gratings are with 65.5 and 70.5 periods, respectively.

CONCLUSION

We proposed a grating system with using Bragg reflector to improve the Smith-Purcell free-electron laser. With theoretical analysis and particle-in-cell simulation, we demonstrated that the interaction of electron beam and wave could be enhanced, and then the growth rate was possibly to be improved.

ACKNOWLEDGEMENT

This work is supported partly by Kurata Grant (1032), KAKENHI (20656014), and Grant-in-Aid for Scientific Research on Innovative Areas “Electromagnetic Metamaterials” (No. 22109003) from The Ministry of Education, Culture, Sports, Science, and Technology (MEXT), Japan. The authors gratefully acknowledge helpful discussions with C.A. Brau.

REFERENCES

[1] J. Gardelle, P. Modin, and J. T. Donohue, Phys. Rev. Lett. **105**, 224801 (2010)
[2] Zh. S. Gevorkian, Phys. Rev. ST Accel. Beams **13**, 070705 (2010)
[3] Amit S. Kesar, Phys. Rev. ST Accel. Beams **13**, 022804 (2010)
[4] J. D. Jarvis, H. L. Andrews, and C. A. Brau, Phys. Rev. ST Accel. Beams **13**, 020701 (2010)
[5] J. Gardelle, L. Courtois, P. Modin, and J. T. Donohue, Phys. Rev. ST Accel. Beams **12**, 110701 (2009)
[6] H. L. Andrews, C. A. Brau, J. D. Jarvis, C. F. Guertin, A. O’Donnell, B. Durant, T. H. Lowell, Phys. Rev. ST Accel. Beams **12**, 080703 (2009)
[7] Vinit Kumar and Kwang-Je Kim, Phys. Rev. ST Accel. Beams **12**, 070703 (2009)
[8] Yuelin Li, Yin-E Sun, and Kwang-Je Kim, Phys. Rev. ST Accel. Beams **11**, 080701 (2008)
[9] Kwang-Je Kim and Vinit Kumar, Phys. Rev. ST Accel. Beams **10**, 080702 (2007)
[10] G. F. Mkrtchian, Phys. Rev. ST Accel. Beams **10**, 080701 (2007)
[11] J. T. Donohue and J. Gardelle, Phys. Rev. ST Accel. Beams **9**, 060701 (2006)
[12] D. Li, Z. Yang, K. Imasaki, and Gun-Sik Park, Phys. Rev. ST Accel. Beams **9**, 040701 (2006)
[13] Amit S. Kesar, Roark A. Marsh, and Richard J. Temkin, Phys. Rev. ST Accel. Beams **9**, 022801 (2006)
[14] Vinit Kumar and Kwang-Je Kim, Phys. Rev. E **73**, 026501 (2006)
[15] H. L. Andrews, C. H. Boulware, C. A. Brau, and J. D. Jarvis, Phys. Rev. ST Accel. Beams **8**, 110702 (2005)
[16] J. T. Donohue and J. Gardelle, Phys. Rev. ST Accel. Beams **8**, 060702 (2005)
[17] D. Li, K. Imasaki, X. Gao, Z. Yang, and Gun-Sik Park, Appl. Phys. Lett. 91, 221506 (2007)
[18] D. Li, K. Imasaki, Z. Yang, and Gun-Sik Park,Appl. Phys. Lett. **88**, 201501 (2006)
[19] H. L. Andrews, C. H. Boulware, C. A. Brau, and J. D. Jarvis, Phys. Rev. ST Accel. Beams **8**, 050703 (2005)
[20] Di Jun, Zhu Da-jun, Liu Sheng-gang, Electromagnetic Field Algorithm of the CHIPIC Code, 2005
[21] H L Andrews, C H Boulware, C A Brau, J T Donohue,J Gardelle and J D Jarvis, New Journal of Physics **8,** 289 (2006)

ISBN 978-3-95450-117-5